



ELSEVIER

Contents lists available at ScienceDirect

## Deep-Sea Research I

journal homepage: [www.elsevier.com/locate/dsrI](http://www.elsevier.com/locate/dsrI)Benthic carbon mineralization in hadal trenches: Assessment by in situ O<sub>2</sub> microprofile measurementsF. Wenzhöfer<sup>a,b,\*</sup>, K. Oguri<sup>c</sup>, M. Middelboe<sup>d</sup>, R. Turnewitsch<sup>e</sup>, T. Toyofuku<sup>c</sup>, H. Kitazato<sup>c</sup>, R.N. Glud<sup>e,f,g</sup><sup>a</sup> Max Planck Institute for Marine Microbiology, Celsiusstr.1, D-28359, Bremen, Germany<sup>b</sup> Alfred-Wegener-Institute Helmholtz Center for Polar and Marine Research, Am Handelshafen 12, D-27570, Bremerhaven, Germany<sup>c</sup> Japan Agency for Marine-Earth Science and Technology, Division of Biodiversity, Yokosuka, Kanagawa 237-0061, Japan<sup>d</sup> University of Copenhagen, Marine Biological Section, 3000 Helsingør, Denmark<sup>e</sup> Scottish Association for Marine Science, Oban PA37 1QA, UK<sup>f</sup> University of Southern Denmark, Nordic Centre for Earth Evolution, Odense M-5230, Denmark<sup>g</sup> University of Aarhus, Arctic Research Centre, Aarhus, Denmark

## ARTICLE INFO

## Article history:

Received 23 June 2016

Received in revised form

25 August 2016

Accepted 31 August 2016

Available online 6 September 2016

## Keywords:

Benthic carbon mineralization

Hadal trenches

Deep sea

in situ

Lander technology

O<sub>2</sub> microprofilesBenthic O<sub>2</sub> uptake

## ABSTRACT

Hadal trenches are considered to act as depo-centers for organic material at the trench axis and host unique and elevated biomasses of living organisms as compared to adjacent abyssal plains. To explore the diagenetic activity in hadal trench environments we quantified in situ benthic O<sub>2</sub> consumption rates and sediment characteristics from the trench axis of two contrasting trench systems in the Pacific Ocean; the Izu-Bonin Trench underlying mesotrophic waters and the Tonga Trench underlying oligotrophic waters. In situ oxygen consumption at the Izu-Bonin Trench axis site (9200 m;  $746 \pm 103 \mu\text{mol m}^{-2} \text{d}^{-1}$ ;  $n=27$ ) was 3-times higher than at the Tonga Trench axis site (10800 m;  $225 \pm 50 \mu\text{mol m}^{-2} \text{d}^{-1}$ ;  $n=7$ ) presumably reflecting the higher surface water productivity in the Northern Pacific. Comparing benthic O<sub>2</sub> consumption rates measured in the central hadal Tonga Trench to that of nearby (60 km distance) abyssal settings (6250 m;  $92 \pm 44 \mu\text{mol m}^{-2} \text{d}^{-1}$ ;  $n=16$ ) revealed a 2.5 higher activity at the trench bottom. Onboard investigations on recovered sediment furthermore revealed that the prokaryotic abundance and concentrations of phytopigments followed this overall trend (i.e. minimum values at the abyssal site followed by higher values from the Tonga and Izu-Bonin Trenches axis, respectively). Excess <sup>210</sup>Pb profiles suggested that mass-wasting events contributed to the deposition of material enhancing the concentration of organic matter in the central trench as compared to the abyssal settings. Our results complement recent findings from the Challenger deep in the Mariana Trench area, which also revealed elevated diagenetic activity in the central trench underpinning the importance of hadal ecosystems for the deep sea carbon cycling.

© 2016 The Authors. Published by Elsevier Ltd. This is an open access article under the CC BY-NC-ND license (<http://creativecommons.org/licenses/by-nc-nd/4.0/>).

## 1. Introduction

Covering the depth range from 6500 to 11000 m, the 27 recognized hadal trenches represent some of the most remote and scarcely studied environments on Earth. Trenches are associated to oceanic faults formed during tectonic subductions and cover about 1–2% of the ocean bed, with the most prominent examples located in the West Pacific (Jamieson, 2015). Trench systems cover a large variety of surface production regimes, ranging from eutrophic (e.g. Atacama Trench) over mesotrophic (e.g. Japan and Izu-Bonin

Trench) to oligotrophic areas (e.g. Mariana Trench and Tonga Trench). While temperature, salinity, O<sub>2</sub> availability and current regimes resemble conditions at the abyssal plain, hadal communities are exposed to extreme hydrostatic pressure and host many specialized piezophile organisms (Somero, 1992; Delong et al., 1997; Jamieson et al., 2010; Kato, 2011; Nunoura et al., 2015). Furthermore, the distinct bathymetry and isolation of the respective hadal basins facilitate endemism and the development of unique trench-associated benthic communities that tends to be of low diversity (Danavaro et al., 2002; Todo et al., 2005; Blankenship et al., 2006; Kitahashi et al., 2013; Fujii et al., 2013; Leduc et al., 2016). However, in contrast to the general food scarcity of the deep sea, hadal trenches were early on recognized as potential depo-centers for organic material at the trench bottom accommodating relatively high abundance and biomass of macro- and meiofauna

\* Corresponding author at: Alfred-Wegener-Institute Helmholtz Center for Polar and Marine Research, Am Handelshafen 12, D-27570, Bremerhaven, Germany.

E-mail address: [frank.wenzhoefer@awi.de](mailto:frank.wenzhoefer@awi.de) (F. Wenzhöfer).

(e.g. Jumars and Hessler, 1976; Tietjen et al., 1989; Danovaro et al., 2002). Even though the mechanisms remain unclear, lateral transport of material from the surroundings and downslope focusing of labile organic material apparently sustain relatively high biological activity at the bottom of many trenches (Gooday et al., 2010; Danovaro et al., 2003; Turnewitsch et al., 2014; Ichino et al., 2015). In addition mass-wasting events often triggered by earthquakes provide large amounts of sedimentary material enriched by carrion-falls to the trench bottom (Nozaki and Ohta, 1993; Itou et al., 2000; Oguri et al., 2013). Trenches thus represent extreme environments and their axis may thereby act as quantitatively important hot spots for deposition and microbial mineralization of organic material in the deep sea.

Exploration of hadal trenches is often associated with great logistic challenges and the requirement of specialized equipment

(Jamieson et al., 2009; Glud et al., 2013; Cui et al., 2014; Gallo et al., 2015) and samples from great depth are prone to recovery artefacts (Tamburini et al., 2013). This is especially true for sediment samples that exhibit a distinct transient increase in microbial activity upon recovery, presumably as a result of DOC enrichment from the lysing of pressure- and temperature-sensitive organisms enhancing metabolism of more resilient organisms (Glud et al., 1994, 1999; Hall et al., 2007). However, recently in situ measurements documented enhanced benthic  $O_2$  consumption rates at  $\sim 11000$  m water depth in the Challenger Deep of the Mariana Trench as compared to nearby abyssal settings reflecting intensified diagenetic activity in the trench axis sediment (Glud et al., 2013). These observations were supported by proxy measurements in recovered sediment cores indicating enhanced deposition of organic material at the trench bottom (Glud et al., 2013).

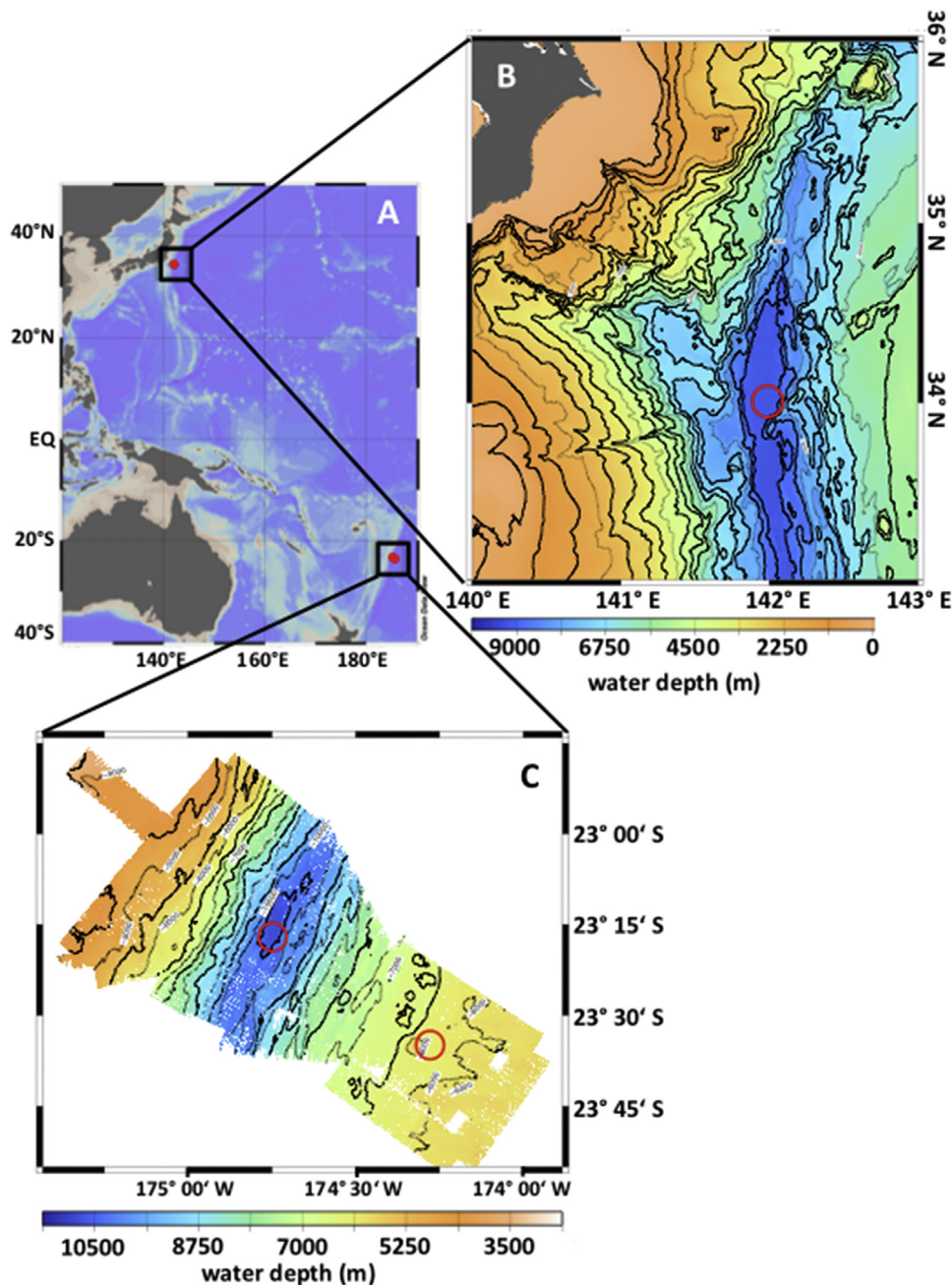


**Fig. 1.** (A) Deployment sites of the two trench systems investigated; Izu-Bonin Trench in the Northern Pacific and Tonga Trench in the Southern Pacific. Close up bathymetry maps of the (B) northern part of the Izu-Bonin Trench and (C) Tonga Trench and abyssal plain sampling locations (Bathymetry maps provided by JAMSTEC).

Here we present in situ benthic O<sub>2</sub> consumption rates as measure of benthic carbon mineralization in trench axis sediments in two contrasting Pacific trench systems underlying water columns of different pelagic productivity: the Tonga Trench and the Izu-Bonin Trench – and for reference abyssal measurements conducted in the vicinity of the Tonga Trench. The in situ work is complemented by measurements of organic carbon content, excess <sup>210</sup>Pb, microbial abundance and proxies for the lability of the organic material in recovered sediment cores. Data are used to discuss and elucidate the potential of stimulated deposition and diagenetic activity in hadal settings.

## 2. Material and methods

### 2.1. Study sites

The northern part of the Izu-Bonin Trench was visited in June 2012 with the RV Yokosuka (YK 12-09). The Izu-Bonin Trench comprises one of the largest hadal benthic habitats as the trench stretches for a length of 1100 km with a width between 5 and 16 km and has a maximum water depth of 9700 m (Jamieson, 2015; Renard et al., 1987). The targeted station of the trench axis was located in the northern section close to the triple junction between Japan Trench, Izu-Bonin Trench and Sagami Trough at a water depth of 9200 m (Ogawa et al., 2008; Fig. 1, Table 1 and Supplementary Table S1).

The ~10800 m deep, central Tonga Trench and a close-by abyssal reference site at ~6250 m were visited during October 2013 also using the RV Yokosuka (YK 13-10), (Fig. 1, Table 1 and Supplementary Table S1). The Tonga Trench axis extends from approx. 15 to 25 °S stretching for a length of 1250 km (Jamieson, 2015). It host the second deepest spot on earth, the Horizon Deep with a water depth of 10890 m (Fisher, 1954; Belyaev, 1989).

The annual average Net Primary Production (NPP) in the two targeted Pacific trenches was assessed from 10 years (1998–2007) of remote sensing data (SeaWiFS; ([http://dx.doi.org/10.5067/ORBVIEW-2/SEAWIFS\\_OC.2014.0](http://dx.doi.org/10.5067/ORBVIEW-2/SEAWIFS_OC.2014.0)) as derived by the Vertical Generalized Production Model of Behrenfeld and Falkowski (1997). The Izu-Bonin Trench site exhibited a relatively high NPP of 200 g C m<sup>-2</sup> yr<sup>-1</sup>, while the value for the Tonga Trench amounted to 106 g C m<sup>-2</sup> yr<sup>-1</sup>. The abyssal reference site was only 60 km from the central Tonga Trench and was within the same province of surface primary production. Unfortunately reference-site measurements off the Izu-Bonin Trench were abandoned due to an incoming typhoon that cut the cruise short. At all three stations we twice deployed instrumentation for in situ measurements of benthic O<sub>2</sub> microprofiles and recovered 6–9 sediment cores for

complementary investigations using either an autonomous sediment sampler or the submersible Shinkai6500 (JAMSTEC, Japan).

### 2.2. Transecting microprofiling lander

Oxygen microprofiles were measured with an ultra-deep diving lander system (Glud et al., 2013). The lander consisted of three components: (I) floatation in the form of 21 units of syntactic foam floats (Custom made, Yokohama Rubber, Japan), (II) an acoustic release system (SB-1010, OKI Electric Industry, Japan), and (III) a basic frame holding a custom build microprofiling system, deep sea battery (Deep Sea Power and Light, US) and ballast weights. The microprofiling unit consisted of the pressure-stable electronic cylinder containing sensor amplifier, data logger and control board, and two sledge systems for horizontal stepping and vertical transecting of the electronic cylinder (Glud et al., 2009).

The base of the pressure cylinder was equipped with 8 sensors for recording vertical depth profiles of O<sub>2</sub>. After descent, the lander remained in a “sleep-mode” for about 1–2 h before the pre-programmed measuring routine was initiated. During the measuring cycles the electronic cylinder with the sensors moved vertically in steps of 500 μm (Izu-Bonin Trench) and 250 μm (Tonga Trench) for a total distance of 20–30 cm. At each position the sensors equilibrated for 5 s before the signal was internally stored. After completing the vertical profile the cylinder with the sensors were moved back to the start position. The electronic cylinder was subsequently moved horizontally for 5.5 cm (Izu-Bonin Trench) and 15 cm (Tonga Trench) and the routine for vertical profiling was re-initiated. This procedure was repeated 7-times at the Izu-Bonin Trench and 5-times at the Tonga Trench.

The pressure-stable cylinder was at each deployment equipped with 8 custom build Clark-type O<sub>2</sub> microelectrodes (Revsbech, 1989). The sensors had a 10–15 cm long slender tip region, and a tip diameter of ~100 μm but a small sensing hole of only 1 μm. This construction combined a rugged design for deep profiling with the advantage of microsensing i.e. stirring sensitivity <1% and a response time of ~0.5 s (Revsbech, 1989; Gundersen et al., 1998). With 8 sensors and 5–7 measuring cycles at each deployment we had hoped to obtain numerous profiles for calculating the benthic O<sub>2</sub> uptake rate and to investigate potential microscale variation in O<sub>2</sub> availability across the sediment water interface as previously done for deep margin sediments (Glud et al., 2005, 2009). However, the sediments contained manganese nodules and stones, which appeared to be sunken pumice, and anecdotally we actually observed many floating pumice in the Tonga Trench area. This combined with the deep penetration of the sensors caused damage to most sensors during the initial profiles and we only obtained between 1 and 24 O<sub>2</sub> microprofiles per deployment. The sensor signal was linearly calibrated against values measured in the bottom water with known O<sub>2</sub> concentrations and on-board determination of the zero-current in anoxic, dithionate-spiked seawater or alternatively against low constant signals in deep-layered sediment that was presumed to be anoxic. Bottom water samples were recovered by Niskin bottles mounted either on the profiling-lander, the camera-coring-lander or the submersible (see below) and the O<sub>2</sub> concentration was determined by Winkler titration (Grasshoff, 1983). The diffusive oxygen uptake (DOU) was calculated from the linear O<sub>2</sub> gradients resolved just below the sediment surface using Fick’s first law of diffusion:  $DOU = \Phi D_s (dC/dz)$  where  $\Phi$  is the measured porosity,  $D_s$  is the tortuosity corrected diffusion coefficient in the sediment,  $C$  is the solute concentration and  $z$  is the sediment depth (Berner, 1980). The  $D_s$  was derived from  $D_s = D_0 \Theta^{-2}$  where  $D_0$  is the temperature and salinity corrected molecular diffusion coefficient of O<sub>2</sub> and  $\Theta$  is the tortuosity derived from the relationship  $\Theta = 1 - \ln(\Phi^2)$  (Boudreau, 1997).

**Table 1**  
Station characteristics.

	Izu-Bonin Trench		Tonga Trench	
	Hadal Site	Abyssal Site	Hadal Site	Abyssal Site
<b>Water depth (m)</b>	9200	–	10800	6250
<b>Bottom water</b>				
– Temperature (°C)	2.2	–	2.0	1.2
– Salinity	34.7	–	34.7	34.8
– Oxygen (μM)	164 ± 4	–	223 ± 3	218 ± 2
<b>Sediment (0–5 cm):</b>				
– Porosity	0.87 ± 0.03	–	0.85 ± 0.04	0.80 ± 0.07
– Dry-sediment density (g cm <sup>-3</sup> )	1.76 ± 0.23	–	1.32 ± 0.04	1.20 ± 0.01
<b>Net Primary Production (NPP)</b>				
mol C m <sup>-2</sup> yr <sup>-1</sup>	16.7 (200)		8.8 (106)	
(g C m <sup>-2</sup> yr <sup>-1</sup> )				

### 2.3. Sediment sampling

For the recovery of intact sediment cores and to obtain video recordings of the seabed an autonomous sediment sampler lander system (Murashima et al., 2009) was deployed 3-times in the Izu-Bonin Trench and 2-times in the Tonga Trench (Supplementary Table S1). The lander system consisted of a floatation system similar to the one used by the profiling lander, a ballast release system and an instrumental payload. A HDTV camera provided continuous 3–8 h long video recordings of the seabed during each of the respective deployments while a conductivity, temperature and depth (CTD) instrument (SBE49, Sea-Bird Electronics, US) recorded basic physico-chemical conditions during the entire deployment. In addition one core liner (id 7.2 cm) was attached to each of the three legs of the tripod. The liners were inserted in the seabed just after landing and in concert with the ballast release the top and bottom of the liners were closed by a spring-loaded system (Murashima et al., 2009). Thus three intact sediment cores were recovered per deployment and divided for further onboard sampling and analyses. Here we report data as obtained from 4–5 sediment cores from each of the two trenches. At the abyssal reference site we obtained 4 push cores (id 4.2 cm) as collected during the dive #1370 by Shinkai6500. In all instances, the recovered sediment cores were sliced in 1 cm sections for the upper 10 cm and into 2 cm sections for the rest of the core length. The sediment was sub-sampled and preserved for subsequent analyses in our respective laboratories.

### 2.4. Quantification of phytopygment concentration

From each sediment section, samples for sediment-bound chlorophyll *a* (Chl *a*) and its degradation products, phaeopigments, were taken by small plastic liners (inner diameter 1.2 cm) and frozen at  $-18^{\circ}\text{C}$  until analysis. Here the sediment was ground and pigments were extracted in acetone (90%) for 24 h. Subsequently samples were centrifuged, and concentrations of Chl *a* and phaeopigments were determined in the supernatant using a Turner fluorometer (Shuman et al., 1975). The ratio of Chl *a*/(Chl *a* + phaeopigments) was used as an indicator for the freshness of the settling material (Pastor et al., 2011).

### 2.5. Quantification of prokaryotic abundance

For extraction of prokaryotes, 1 mL of homogenized sediment from selected depth intervals were transferred to 50 mL centrifuge tubes and fixed with 1 mL 1% glutaraldehyde. Then, 5 mL of 5 mM  $\text{Na}_4\text{P}_2\text{O}_7$  was added and the samples were sonicated for 20 s on ice (3 cycles at 20 kHz) (Danovaro and Middelboe, 2010). The samples were then further diluted with 40 mL Milli-Q water and sub-samples of 2 mL were transferred to cryovials, snap frozen in liquid nitrogen and stored at  $-80^{\circ}\text{C}$  until analysis of prokaryote abundance. Here samples were 10-times diluted in TE buffer (10 mM Tris, 1 mM EDTA [pH 8.0]) and stained with SYBR green I (Molecular Probes, Invitrogen Inc., Life Technologies, NY). Cell abundance was quantified using flow cytometry (BD FACS Canto) equipped with an air-cooled argon laser (excitation wavelength, 488 nm) (Carreira et al., 2015).

### 2.6. Measurements of porosity, density and organic carbon content

For basic sediment characteristics 10–15 mL of sediment from the respective sections were stored frozen ( $-18^{\circ}\text{C}$ ). In the home laboratory, the sediment was thawed and thoroughly homogenized. The sediment water content was determined as the relative weight loss after drying to constant weight at  $105^{\circ}\text{C}$  and porosity was calculated accounting for the measured density.

Homogenized samples were weighed into silver containers and pretreated with 6 M HCl to dissolve any carbonate. The organic carbon content was measured in CNS-analyzers (Izu-Bonin-Trench samples: Costech ECS4010; Tonga-Trench samples: Fisions NA 1500, Series 2) by flash combustion (Verado et al., 1990).

### 2.7. Measurements of $^{214}\text{Pb}$ , $^{137}\text{Cs}$ and $^{210}\text{Pb}$

Methods for the determination of excess  $^{210}\text{Pb}$  ( $^{210}\text{Pb}_{\text{ex}}$ ) in sediments are described in Glud et al. (2013) and Turnewitsch et al. (2014). Sediment samples were first stored at  $+5^{\circ}\text{C}$ . For analyses, the samples then were dried at  $80^{\circ}\text{C}$  for 48 h, milled and subsamples of 2 g were stored in hermetic sealed plastic tubes for 2 months. Total (i.e. sum of supported and excess)  $^{210}\text{Pb}$ ,  $^{214}\text{Pb}$  and  $^{137}\text{Cs}$  concentrations were measured using a 12030 well-type germanium gamma ray detector (ORTEC, US) and an APV8002 multi-channel spectrum analyzer (Techno AP, Japan), with a background value of the detector of  $0.0094\text{ Bq g}^{-1}$  for  $^{210}\text{Pb}_{\text{ex}}$ . The results of the sediment cores occasionally expressed a higher but constant value of  $\sim 0.05\text{ Bq g}^{-1}$  in deeper sediment layers. We currently have no satisfactory explanation for these low apparent excess activities. However, as their influence on inventories and the interpretation of the main results is very small we thought it justified not to discuss them in this paper. The counting time for the measurements was 1–2 days. The respective peak areas of the raw data of  $^{210}\text{Pb}$  ( $T_{1/2}=22.3\text{ y}$ ; 46.5 keV) and  $^{214}\text{Pb}$  (351.9 keV) and  $^{137}\text{Cs}$  ( $T_{1/2}=30\text{ y}$ ; 661.6 keV) were calculated by Gaussian curve fitting using KaleidGraph 4.1.  $^{210}\text{Pb}_{\text{ex}}$  activities were obtained by subtracting  $^{214}\text{Pb}$  activities from the total  $^{210}\text{Pb}$  assuming secular equilibrium between  $^{226}\text{Ra}$  and the short-lived daughters, including  $^{214}\text{Pb}$  in the sediment. As reference material for  $^{210}\text{Pb}$  and  $^{214}\text{Pb}$  we applied DL-1a Uranium-Thorium ore ( $1.40 \pm 0.02\text{ Bq g}^{-1}$  in  $^{210}\text{Pb}$ ; Natural Resources, Canada) and for  $^{137}\text{Cs}$ , we applied IAEA 375 soil ( $5.280 \pm 0.06\text{ Bq g}^{-1}$ , determined on 31 Dec. 1991; IAEA).

## 3. Results

### 3.1. Video recordings

The sediment surface at the Izu-Bonin and Tonga Trench axis as well as the abyssal plain in the vicinity of the Tonga Trench appeared similar with little disturbance and conspicuous fauna at the sediment surface (not shown). However, lebensspuren were visible at the sediment surface (Supplementary Fig. S1), and at all sites scavenging amphipods (*Hirondellea* sp.) appeared abundant and several specimens were caught on lander-mounted traps. Amphipods appeared more abundant in the trench settings. The video recording showed that amphipods frequently emerged from and retreated to the sediment and this activity presumably resulted in efficient particle mixing in the surface layer. The recovered sediment cores of the present study were not investigated for macrofauna in any great detail, but no conspicuous infauna was observed during core slicing.

### 3.2. $\text{O}_2$ microprofiles

In total we successfully obtained 50  $\text{O}_2$  microprofiles and none of these reflected presence of infauna burrows or fauna induced irrigation. At all three locations the sediment surface was well oxygenated with an extensive  $\text{O}_2$  penetration depth (OPD) (Fig. 2). However, the abyssal site clearly exhibited the deepest OPD exceeding the maximum measuring depth of our microsensors ( $\sim 13\text{ cm}$ ). Applying a linear extrapolation of the concentration profiles at the abyssal Tonga Trench site provided a minimum OPD of  $\sim 50\text{ cm}$ . The OPDs at the two trench axis sites were

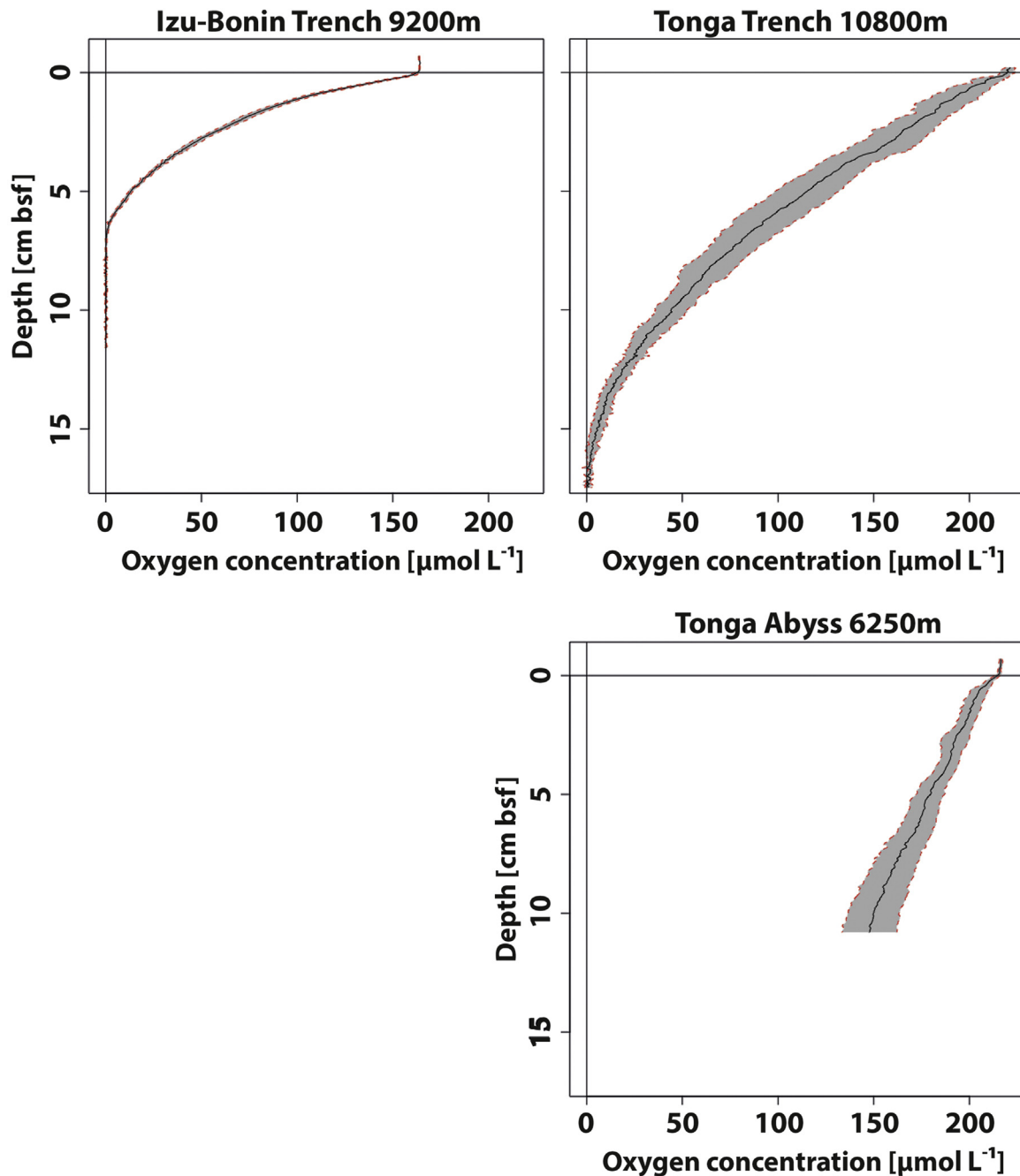


**Fig. 2.** Average in situ benthic  $O_2$  profiles measured at the two trench systems with their 95% confidence interval. (A) At the Izu-Bonin Trench site at 9200 m water depth 27  $O_2$  microprofiles were measured; (B) at the Tonga Trench site at 10800 m water depth 7 profiles were measured, (C) while at the Tonga abyssal site at 6250 m water depth 16 profiles were recorded. The horizontal line represents the sediment-water interface and the depth is given as centimeter below seafloor.

significantly shallower reflecting higher benthic  $O_2$  consumption rates (Fig. 2). The sediment of the Tonga Trench bottom provided an intermediate OPD of  $16.1 \pm 1.0$  cm ( $n=7$ ), while the shallower and more eutrophic site in the Izu-Bonin Trench showed an OPD of  $6.4 \pm 0.3$  cm ( $n=27$ ) (Fig. 2, Table 2). The calculated benthic  $O_2$  consumption rates reflected the differences in OPD, with the lowest metabolic activity of  $92 \pm 44$   $\mu\text{mol m}^{-2} \text{d}^{-1}$  ( $n=16$ ) at the Tonga abyssal plain,  $225 \pm 50$   $\mu\text{mol m}^{-2} \text{d}^{-1}$  ( $n=7$ ) within the Tonga Trench and the highest activity of  $746 \pm 103$   $\mu\text{mol m}^{-2} \text{d}^{-1}$  ( $n=27$ ) at the Izu-Bonin Trench axis. (Fig. 2, Table 2). The scatter seen in the averaged profiles from the Tonga Trench axis (Fig. 2(B)) and abyssal (Fig. 2(C)) site most likely result from the small stones observed in these sediments.

### 3.3. Sediment parameters

#### 3.3.1. Organic carbon and phytopigments

The total organic carbon content at the three sites was similar, with depth integrated values (0–15 cm) ranging around  $\sim 6.0$ – $6.5$   $\text{kg m}^{-2}$  (Table 2). At the Tonga area both the abyssal and hadal stations exhibited relatively constant organic carbon content throughout the sediment core indicating relatively well-mixed sediments (Fig. 3(B)). In contrast, the sediment surface at the Izu-Bonin Trench site appeared enriched in organic material, and relatively little variability was observed at sediment depths  $> 5$  cm (Fig. 3(A)).

In contrast to the total organic material the concentrations of

**Table 2**

Benthic fluxes and depth-integrated sediment parameter from hadal and abyssal trench sites; oxygen uptake and oxygen penetration depth (OPD) as derived from in situ microprofiles; depth-integrated values from retrieved sediment cores.

	<b>O<sub>2</sub> uptake</b> ( $\mu\text{mol m}^{-2} \text{d}^{-1}$ )	<b>OPD (cm)</b>	<b>Organic C content<sup>a</sup></b> ( $\text{g m}^{-2}$ )	<b>Chl a<sup>a</sup></b> ( $\text{mg m}^{-2}$ )	<b>Phaeophytin<sup>a</sup></b> ( $\text{mg m}^{-2}$ )	<b>Ratio Chl a/(Chl a + phaeophytin) (%)</b>	<b>Prokaryotic abundance<sup>a</sup></b> ( $\text{cells cm}^{-2}$ )	<b><sup>210</sup>Pb<sub>ex</sub> inventory<sup>b</sup></b> ( $\text{kBq m}^{-2}$ )
<b>Izu-Bonin Trench</b>								
hadal	746 ± 103 (n=27)	6.4 ± 0.3 (n=27)	6013 ± 309	217 ± 23 (n=4)	625 ± 181 (n=4)	27 ± 4.7 (n=4)	76 × 10 <sup>7</sup> ± 2.5 × 10 <sup>7</sup>	40.5 <sup>c</sup> ± 4.3
abyssal	n.d.	n.d.	n.d.	n.d.	n.d.	–	n.d.	n.d.
ratio	–	–	–	–	–	–	–	–
<b>Tonga Trench</b>								
hadal	225 ± 50 (n=7)	16.1 ± 1 (n=7)	6119 ± 889	29 ± 1.8 (n=2)	125 ± 43.8 (n=2)	20 ± 6.5 (n=2)	12 × 10 <sup>7</sup> ± 0.14 × 10 <sup>7</sup>	207.6 ± 3.6
abyssal	92 ± 44 (n=16)	n.d.	6663 ± 36	4.5 ± 0.3 (n=2)	21 ± 3.7 (n=2)	18 ± 1.6 (n=2)	7.2 × 10 <sup>7</sup> ± 0.13 × 10 <sup>7</sup>	9.5 ± 4.6
ratio	2.5	–	0.9	6.4	5.9	1.1	1.7	21.8
<b>Mariana Trench<sup>d</sup></b>								
hadal	154 ± 48 (n=51)	n.d.	707	0.4	1.5	21	14 × 10 <sup>7</sup> ± 2.4 × 10 <sup>7</sup>	50.5 ± 8.0
abyssal	85 ± 38 (n=36)	n.d.	629	0.1	0.6	14	2.4 × 10 <sup>7</sup> ± 1.2 × 10 <sup>7</sup>	17.9 ± 0.9
ratio	1.8	–	1.1	4	2.5	1.5	5.8	2.8

<sup>a</sup> Depth-integrated values (0–15 cm).

<sup>b</sup> Depth-integrated over the entire core length.

<sup>c</sup> Derived from Turnewitsch et al. (2014).

<sup>d</sup> Recalculated or derived from Glud et al. (2013).

phytopigments were distinctly different at the three stations. The depth-integrated values of phytopigments (0–15 cm) at the Izu-Bonin site were ~5-times higher than in the Tonga Trench which again were ~5-times higher than the values from the neighboring abyssal plain (Table 2). At the Tonga Trench sites no clear sediment-depth trend was visible, except for a potential minor peak of phaeopigments at the trench site at 5 cm depth (Fig. 3(D)). The Chl a and phaeopigment concentrations in surface sediments at the Izu-Bonin Trench were higher than at the Tonga sites and the concentration decreased with depth over the first 7 cm, before sharply increasing within 2 cm and reaching an elevated value that remained relatively constant to the bottom of the core (Fig. 3(C)).

### 3.3.2. Abundance of prokaryotic cells

The highest depth-integrated prokaryotic abundance was found at the Izu-Bonin Trench hadal site with  $7.6 \times 10^8$  cells  $\text{cm}^{-2}$ , followed by the hadal Tonga Trench site ( $1.2 \times 10^8$  cells  $\text{cm}^{-2}$ ) and the abyssal Tonga site ( $7.2 \times 10^7$  cells  $\text{cm}^{-2}$ ) (Table 2). As for the concentration of phytopigments and the organic carbon content, both Tonga sites exhibited a relatively constant abundance of prokaryotes from the surface to the bottom of the core (Fig. 3(F)). At the Izu-Bonin site the prokaryotic abundance exhibited a distinct shift to elevated values at 7 cm depth (Fig. 3(E)), mirroring the profile structure of the phytopigment concentration presented above (Fig. 3(C)).

### 3.3.3. Sediment profiles of <sup>210</sup>Pb<sub>ex</sub> and <sup>137</sup>Cs profiles

The excess <sup>210</sup>Pb (<sup>210</sup>Pb<sub>ex</sub>) activity near the sediment-water interface of the Izu-Bonin Trench axis was ~3-times higher than at the Tonga Trench axis (Fig. 3(G) and (H)). But in contrast to the Tonga Trench the values in the Izu-Bonin Trench exhibited a strong monotonous decrease in activities from the sediment-water interface down to ~6–7 cm sediment depth (Fig. 3(G)). This depth coincided also with distinct shifts in the sediment profiles of prokaryote abundance and phytopigment concentrations (Fig. 3(C) and (E)). The depth-integrated inventory at the hadal Izu-Bonin Trench site (~40 kBq  $\text{m}^{-2}$ ) was ~5-times lower than at the hadal Tonga Trench site (~200 kBq  $\text{m}^{-2}$ ) (Table 2). The surface activity of <sup>210</sup>Pb<sub>ex</sub> in the Tonga Trench hadal site was ~4-times higher than at the abyssal reference site (Fig. 3(H)). This to a minor extend

is due to the depth effect on specific <sup>210</sup>Pb<sub>ex</sub> activities and inventories. The specifics of the profile shapes and the environmental settings, however, indicate that the difference in this particular case is mainly due to (1) a relatively recent turbiditic deposit in the trench axis and (2) moderate topographically (abyssal-hill) controlled reduction of deposition at the abyssal trench-rim site. Furthermore, while the activity at the abyssal site quickly reached an almost constant lower value, the values at the hadal trench site remained elevated down to the maximum measuring depth of 20 cm. The depth-integrated <sup>210</sup>Pb<sub>ex</sub> inventory from the hadal Tonga Trench was extremely high and showed ~20-fold higher values (207 kBq  $\text{m}^{-2}$ ) than the abyssal site (~10 kBq  $\text{m}^{-2}$ ) (Table 2). The depth integrated <sup>210</sup>Pb<sub>ex</sub> values at the hadal site would presumably have been even higher if it had been possible to obtain longer sediment cores as values remained elevated to the bottom of the core (Fig. 3(H)).

No <sup>137</sup>Cs was detected in the Tonga Trench area, probably reflecting low flux of <sup>137</sup>Cs to the southern hemisphere during the nuclear weapons tests in 1945–1963 (Tsumune et al., 2011). However, at the Izu-Bonin Trench, <sup>137</sup>Cs penetrated to 4–5 cm sediment depth (Supplementary Fig. S2). No <sup>134</sup>Cs ( $T_{1/2}=2.06$  y, 605 and 796 keV) was encountered in any of our samples; this contrasts with <sup>134</sup>Cs that was previously observed at 7261 m depth in Japan Trench and being ascribed to leakage during the 2011 Fukushima Dai-ichi nuclear power plant accident (Oguri et al., 2013).

## 4. Discussion

The diagenetic efficiency of marine sediments regulates the long-term regeneration and the preservation of organic material and therefore plays an important role for oceanic element cycling (e.g. Canfield, 1994; Wollast, 1998). One of the most robust and widely applied proxies for benthic carbon mineralization is to quantify the benthic O<sub>2</sub> consumption rate (Glud, 2008). In coastal settings, irrigation and respiration by fauna can contribute significantly to the degradation efficiency and activity (Kristensen, 1988; Aller 1994; Wenzhöfer and Glud, 2004). However, the relative importance of fauna attenuates with water depth, and at deep sea settings the diagenetic activity is almost exclusively mediated by the microorganisms (Glud et al., 1994; Wenzhöfer

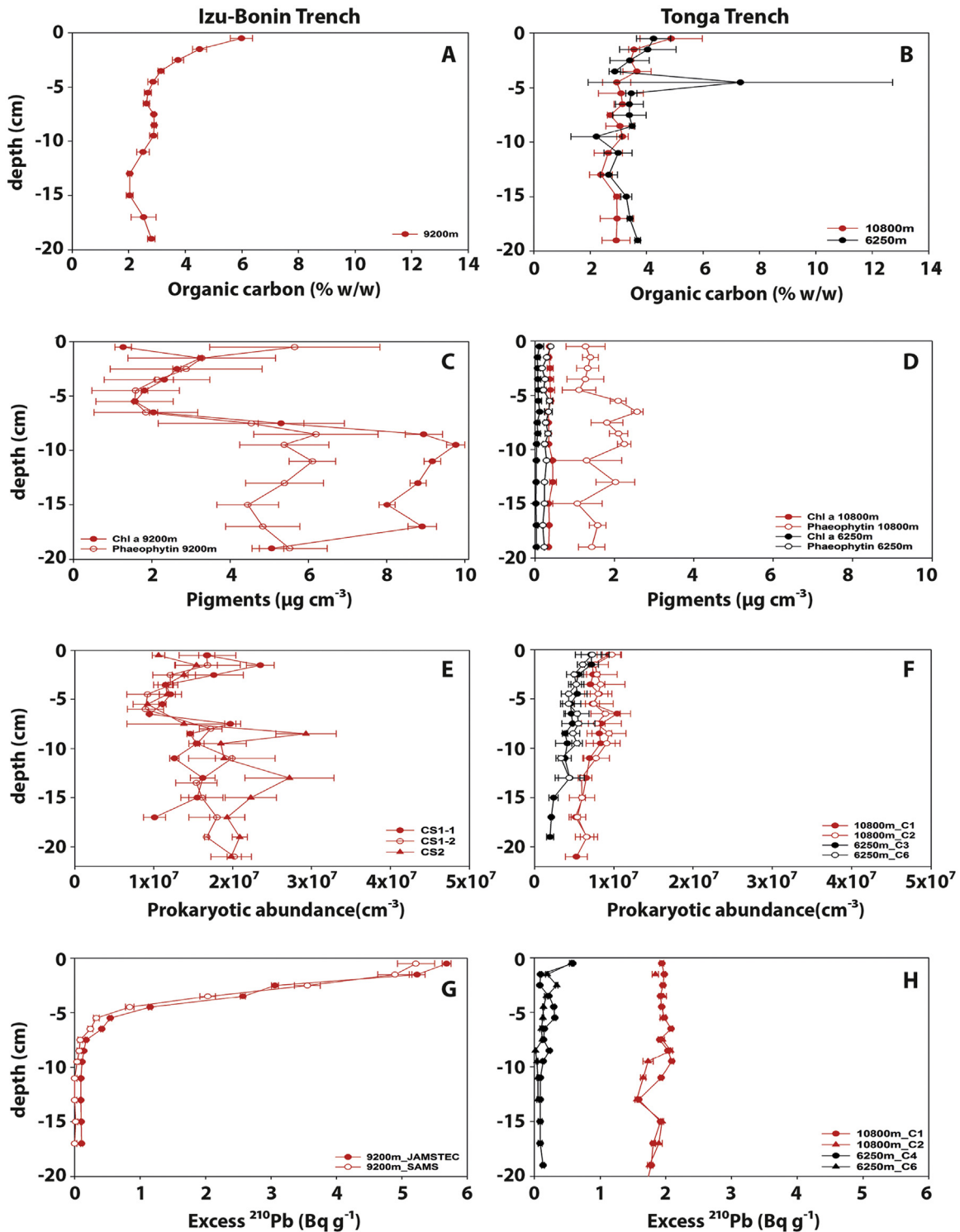


**Fig. 3.** Sediment characteristics of the two trench systems; (A and B) organic carbon content of the sediment; (C and D) pigment concentrations as chlorophyll a (Chl a) and phaeophytin; (E and F) prokaryotic abundance; (G and H) excess  $^{210}\text{Pb}$ . Hadal sites shown in red and abyssal sites shown in black. (For interpretation of the references to color in this figure legend, the reader is referred to the web version of this article.)

and Glud, 2002; Glud, 2008). Therefore, the diffusive mediated  $\text{O}_2$  uptake (DOU) as derived from pore water microprofiles provides a good measure for the total turnover of organic material in abyssal and hadal sediments. Overall the benthic  $\text{O}_2$  uptake gradually declines by  $\sim 3\text{--}4$  orders of magnitude moving from coastal settings to abyssal water depths with  $\text{O}_2$  fluxes decreasing from roughly  $50 \text{ mmol m}^{-2} \text{ d}^{-1}$  down to  $0.1\text{--}0.5 \text{ mmol m}^{-2} \text{ d}^{-1}$  (Andersson et al., 2004; Glud, 2008, Fig. 4). However, low biological

activity with extremely low  $\text{O}_2$  uptake rates of  $0.1\text{--}0.3 \text{ mmol m}^{-2} \text{ d}^{-1}$  are encountered in sediments of the central ocean gyres, due to the extremely low flux of particulate organic matter from the photic zone to the seafloor (Fischer et al., 2009; Murray and Grundmanis, 1980). Despite the relatively low biogeochemical activity of deep sea sediments they are still estimated to be responsible for  $> 50\%$  of the global benthic carbon mineralization due to their vast extent (e.g. Jahnke, 1996; Andersson

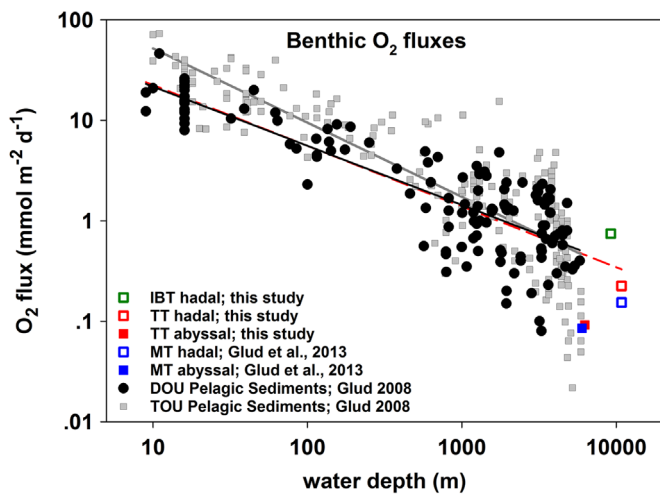


**Fig. 4.** Global benthic  $O_2$  fluxes as function of water depth. Data for pelagic sediments on dissolved oxygen uptake (DOU; dark circles) and total oxygen uptake (TOU; grey squares) are taken from Glud (2008). The corresponding linear relationships are  $DOU = 84x^{-0.59}$  ( $R^2 = 0.74$ ) and  $TOU = 284x^{-0.74}$  ( $R^2 = 0.74$ ), respectively (Glud, 2008). The extended regression for DOU also including the data from trench system studies (red dashed line; Glud et al. (2013) and this study) does not differ much  $DOU = 90.5x^{-0.56}$  ( $R^2 = 0.74$ ). The difference between TOU and DOU can be addressed to fauna-mediated oxygen uptake ( $FOU = TOU - DOU$ ); the relative proportion of FOU decreases with depth. (For interpretation of the references to color in this figure legend, the reader is referred to the web version of this article.)

et al., 2004; Glud, 2008) and correct assessment of deep sea carbon mineralization is important for constraining large scale oceanic carbon cycling.

The depth attenuation of benthic carbon mineralization mainly reflects gradual degradation of sinking organic material and higher pelagic productivity along continental slopes and in coastal waters as compared to the open ocean (Jahnke and Jackson, 1992; Wenzhöfer and Glud, 2002; Glud, 2008). However, available in situ data on benthic carbon degradation in the deep sea settings still vary by almost 2 orders of magnitude (Fig. 4). This is presumed to reflect extensive spatial and temporal variation in surface production (Wenzhöfer and Glud, 2002; Smith et al., 2013), but also variable down slope lateral transport (Jahnke et al., 1990) and focusing of organic material in bathymetrically varied seascapes (e.g. de Stigter et al., 2007; de Leo et al., 2010). Hadal trenches represent the extreme end-member of the oceanic continuum and trench axis sediments are considered to represent major oceanic depo-centers with intensified material loading and elevated abundance of fauna (Danovaro et al., 2003; Tietjen et al., 1989; Jumars and Hessler, 1976; Turnewitsch et al., 2014; Ichino et al., 2015; Leduc et al., 2016), yet their benthic mineralization activity remains largely unexplored.

#### 4.1. Intensified diagenetic activity in hadal trench axis sediments

There only exist few in situ determinations of benthic  $O_2$  consumption rates from the deep abyss. Available data for water depth between 4500 and 6500 m range from 50 to 575  $\mu\text{mol m}^{-2} \text{d}^{-1}$  with an overall average value of  $265 \pm 169 \mu\text{mol m}^{-2} \text{d}^{-1}$  ( $n=20$ ) while the corresponding values for the 5000–6500 m depth interval are 50–356  $\mu\text{mol m}^{-2} \text{d}^{-1}$  with an average of  $175 \pm 128 \mu\text{mol m}^{-2} \text{d}^{-1}$  ( $n=9$ ) (Reimers et al., 1986; Smith et al., 1978; Berelson et al., 1990; Hales et al., 1994; Glud et al., 1994, 2013; Wenzhöfer and Glud, 2002; this study). The three available data sets from hadal depths (>6500 m) range from  $154 \pm 48 \mu\text{mol m}^{-2} \text{d}^{-1}$  in the Mariana Trench ( $\sim 10900$  m),  $225 \pm 50 \mu\text{mol m}^{-2} \text{d}^{-1}$  in the Tonga Trench ( $\sim 10800$  m) up to

$746 \pm 103 \mu\text{mol m}^{-2} \text{d}^{-1}$  in the Izu-Bonin Trench ( $\sim 9200$  m) (Table 2, Fig. 5). The ranking of the values mirrors the estimated pelagic productivity in the respective provinces equaling 4.2, 8.8 and 16.7  $\text{mol C m}^{-2} \text{yr}^{-1}$  in the areas of the Mariana Trench, the Tonga Trench and the Izu-Bonin Trench, respectively (Table 2, Glud et al. (2013)). This suggests a direct link between the regional pelagic productivity and benthic diagenetic activity at the respective hadal trench bottoms. Overall the absolute values of the  $O_2$  consumption of the investigated hadal sediments are similar or even exceed the available data from the deep abyss. Comparison of benthic consumption rates measured in central hadal trenches to those of nearby abyssal settings confirms intensified activities in trench settings that are 1.8–2.5-times higher in the trenches as compared to near-by abyssal sites (Table 2, Fig. 5). The elevated benthic diagenesis is reflected by relatively higher prokaryote (Table 2, Fig. 5, Glud et al. (2013)) and meiofauna abundance in hadal sediments (Danovaro et al., 2002; Leduc et al., 2016). The few available data on prokaryotic abundances in hadal sediments may even be considered to be minimum values given that cell lysis associated to recovery artifacts is expected to be more prominent in deeper settings (Hall et al., 2007). The higher microbial biomass and elevated diagenetic activity must be sustained by an elevated food supply to hadal sediments. But this is not necessarily reflected by higher total organic carbon content of hadal sediments (Fig. 5(B)), which for a large part presumably consist of relatively refractory material. Rather, it could be speculated that the enhanced activity is being sustained by a relatively efficient supply of more labile organic material that only makes up a small part of the sedimentary material.

Using the Chl a/(Chl a + phaeopigments) ratio as an indicator for the freshness of the settling organic material (Stephens et al., 1997; Pastor et al., 2011) indeed indicates that more labile material reaches the trench bottoms than the neighboring abyssal plains (Table 2). It is important to notice that the current investigation target the central basins of the respective trenches and cannot be extrapolated to the entire trench systems. Individual trenches exhibit a great downslope variety of habitats, with steep trench walls and ragged outcrops where sediments can accumulate (Blankenship-Williams and Levin, 2009). There are also places of tectonic activity sustaining biological hot spots based on chemosynthetic communities. While the importance of chemosynthetic organic material produced at seeps or vents in hadal settings remain an unquantified carbon source for hadal communities, the observation of elevated concentration of phytopigments in hadal sediments would still suggest a mechanism for focusing phytodetrital material along the trench axis sustaining elevated microbial activity with labile organic material in the central basins.

It has been suggested that increasing hydrostatic pressure may inhibit mineralization of sinking aggregates that mainly are colonized by microbes from surface waters and that relatively labile unprocessed phytodetrital material may reach great depth (Tamburini et al., 2013). This alone would, however, not explain higher concentration of phytopigments at hadal versus abyssal depths which would require a preferential down slope focusing of phytodetrital material towards the trench axis (Turnewitsch et al., 2014). This could potentially be maintained by frequent suspension and re-deposition of material along the trench slopes that would gradually lead to focusing of detrital material at the sediment surface in the central trench. Tidally driven hydrodynamic forcing and seismic activity could drive such a process. It is well established that earthquakes can trigger mass wasting, down slope transport of sedimentary material, but subsequent aftershocks and instability along the trench slopes can presumably maintain down slope material transport for extensive periods (Itou et al., 2000; Oguri et al., 2013). Dense, 30–50 m thick nepheloid layers were observed in the central Japan Trench four months after the

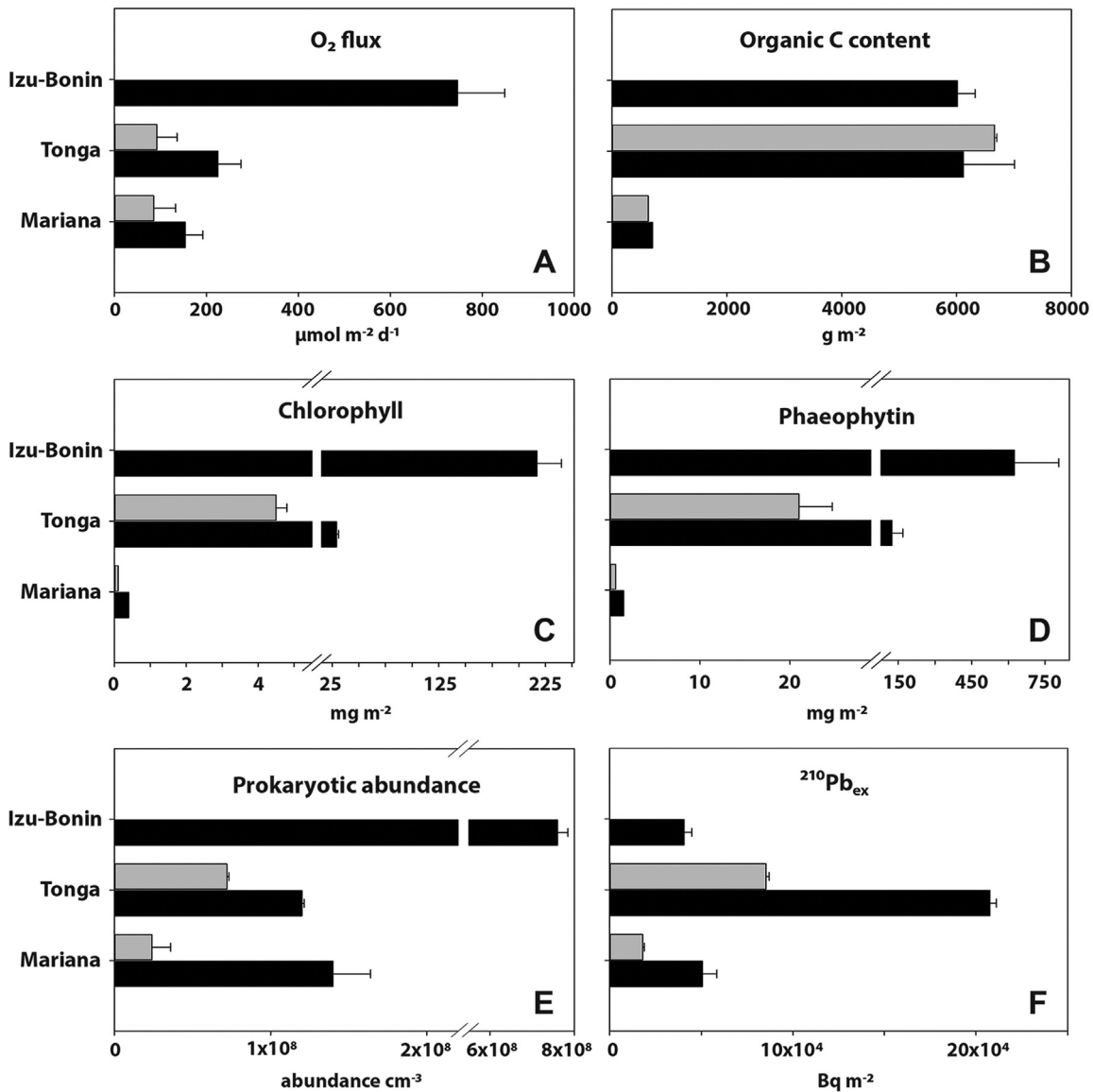


**Fig. 5.** Comparison of benthic O<sub>2</sub> fluxes and sediment compounds (organic carbon content, chlorophyll, phaeophytin, prokaryotic abundance and excess <sup>210</sup>Pb) from the Izu-Bonin trench, Tonga trench and Mariana Trench (Glud et al., 2013) system. Black bars represent hadal sites and grey bars abyssal sites.

Tohoku-Oki Earthquake (Oguri et al., 2013) and this would lead to preferential concentration of light detrital material in the upper sediment layers along the trench axis. Such events are also expected to lead to the deposition of large amounts of macrofauna carrion that will be focused at the trench bottom and sustaining microbial activity for extended periods (Oguri et al., 2013). Detailed investigation of radionuclide distribution in recovered sediment cores can provide some insight on deposition and particle dynamics in the targeted sediments.

#### 4.2. Deposition dynamics as inferred from <sup>210</sup>Pb<sub>ex</sub> and <sup>137</sup>Cs profiles

The radionuclide data together with the other sediment-compositional data suggest that the hadal surface sediments of the trench axis seafloor at both, the Izu-Bonin and the Tonga Trench system, had been affected by mass wasting events, potentially followed by subtle slower post-event processes that gradually smoothed the sediment surface. However, the data also suggest that the timing of the events differed between the two sites.

At the Izu-Bonin Trench the partially lumpy topography of the

surface sediment and the distribution of organic carbon and phytopigments indicate the possible deposition of mass-wasted sediment. The sharp decrease in <sup>210</sup>Pb<sub>ex</sub> reaching low or near-zero levels at 5–6 cm depth (Fig. 3(G)), however, indicates that the most recent mass-wasting event (if any) occurred at least ~100 years ago (5 × <sup>210</sup>Pb half-lives) and that the topmost layer was also affected by a relatively recent gradual biological down mixing. This latter notion is also supported by the <sup>137</sup>Cs results (Supplementary Fig. S2). At 5–6 cm depth the O<sub>2</sub> concentration approached zero, but prokaryotic abundance and phytopigments exhibited a distinct upward shift indicating a very pronounced change in sediment biogeochemistry and possibly sediment provenance. The absence of significant amounts of <sup>210</sup>Pb<sub>ex</sub> in this deeper layer (> 6 cm; Fig. 3(G)) shows that this layer would also have resulted from a mass-wasting event older than ~100 yr.

The <sup>210</sup>Pb<sub>ex</sub> profile in the central hadal Tonga Trench exhibits three distinctive features, i) surface activities (~1.9 Bq g<sup>-1</sup>) that are comparatively low for this water depth, ii) deep penetration and nearly constant values, but iii) an unusual high depth-integrated <sup>210</sup>Pb<sub>ex</sub> inventory (Fig. 3(H); Table 2) with all features

pointing towards a major sediment deposition event in relatively recent time. The surface value is in fact much lower than previously reported for hadal trench surface sediments, with the exception of sediments from the central Izu-Ogasawara Trench (Yamada et al., 1983; Swinbanks and Shirayama, 1986) that are thought to be influenced by very intense intertidal tides that propagate across the trench (Turnewitsch et al., 2014). Hadal trenches are often characterized by large earthquakes inducing turbidity currents and large submarine down slope landslides (Kawamura et al., 2012). These seismic events create thick distinct deposits at the hadal seafloor of the trench axis (Itou et al., 2000; Oguri et al., 2013). In the past five decades, 42 earthquakes over a magnitude of 6.0 were recorded in the investigated area of the Tonga Trench (21.6 °S, 183.3 °W to 24.71 °S, 186.6 °W; U.S. Geological Survey, <http://earthquake.usgs.gov/earthquakes/search/>). Thus the constant  $^{210}\text{Pb}_{\text{ex}}$  activities down to the bottom of the core (Fig. 3(H)) most likely resulted from an event of sudden, intense mass deposition. In the upper sediment layer amphipod behavior, as observed in video records (Supplementary Fig. S1), could have re-started biological sediment mixing after the mass-wasting event (Leduc et al., 2016).

The  $^{210}\text{Pb}_{\text{ex}}$  profile at the abyssal site near the Tonga Trench features low specific  $^{210}\text{Pb}_{\text{ex}}$  activities in the sediment, with slightly elevated values directly at the surface (Fig. 3(H)) and relatively low  $^{210}\text{Pb}_{\text{ex}}$  inventories (Table 2). Such features presumably reflect low vertical deposition of material rather than mass wasting as seen at the hadal trench site. Surprisingly, under similarly oligotrophic surface waters and at a similar water depth, specific activities of  $^{210}\text{Pb}_{\text{ex}}$  in surface sediments of the oceanward rim of the Mariana Trench were up to twice as high ( $1.79 \text{ Bq g}^{-1}$ ) and inventories were up to ~5-times as high than encountered at the Tonga Trench rim (Table 2) (Glud et al., 2013). The sampling site is located close to an abyssal hill and topographically accelerated near-seafloor waters may have led to comparatively low  $^{210}\text{Pb}_{\text{ex}}$  (and sediment) deposition at this particular trench-rim site.

## 5. Conclusion

The overall rates and the relative importance of the different diagenetic pathways at the bottom of hadal trench systems are controlled by the deposition rate of organic matter. The diagenetic activity of the three trenches investigated so far shows that benthic  $\text{O}_2$  consumption rates at the trench axis decrease from Izu-Bonin Trench > Tonga Trench > Mariana Trench according to the productivity of the mesotrophic and oligotrophic surface waters of their respective provinces. However, hadal deposition dynamics at the trench axes are highly variable and mass wasting may significantly affect the amount and the distribution of organic matter in the central trenches. This may induce a temporal dynamic in diagenetic activity at the trench bottoms showing elevated rates after mass wasting events and a subsequent decline in the activity. However, overall trench axes sediments seem to be enriched in food availability, prokaryotic abundance and metabolic activity as compared to adjacent abyssal sites. It can be speculated that even small scale and more frequent mass wasting events in combination with subtle bio-resuspension and tidal flow oscillations can maintain a relatively high diagenetic activity in hadal sediments of trench axes.

## Acknowledgments

We thank the captains and crews of RV Yokusuka expeditions YK 12-09 and YK 13-10 and the pilots of the submersible

Shinkai6500 for their invaluable help with work at sea. Volker Asendorf, Axel Nordhausen, Patrick Meyer are gratefully acknowledged for support with the in situ profiling lander. We thank Anni Glud for electrode constructions, Oscar Chiang for help with flow cytometry, and Martina Alisch and Rafael Stiens for sediment sample processing. The study was financially supported by the Natural Environment Research Council (NERC; NE/F018612/1, NE/F0122991/1, NE/G006415/1), the commission for Scientific Research in Greenland (KVUG; GCRC6507). This study contributes to the project HADES-ERC funded by the European Research Council Advanced Investigator Grant 669947. Additional resources were provided by JAMSTEC, the Helmholtz Association and the Max Planck Society. We thank two anonymous reviewers for their valuable and constructive comments on the manuscript.

## Appendix A. Supporting information

Supplementary data associated with this article can be found in the online version at <http://dx.doi.org/10.1016/j.dsr.2016.08.013>.

## References

- Aller, R.C., 1994. Bioturbation and remineralization of sedimentary organic matter: effects of redox oscillation. *Chem. Geol.* 114, 331–345.
- Andersson, H.J., Wijsman, J.W.M., Herman, P.M.J., Middelburg, J.J., Soetaert, K., Heip, C., 2004. Respiration patterns in the deep ocean. *Geophys. Res. Lett.* 31, L03304.
- Behrenfeld, M.J., Falkowski, P.G., 1997. Photosynthesis rates derived from satellite-based chlorophyll concentration. *Limnol. Oceanogr.* 42, 1–20.
- Belyaev, G.M., 1989. *Deep Sea Ocean Trenches and Their Fauna*. Nauka Publishing House, Moscow, p. 385 (Translated to English by Scripps Institution of Oceanography, USA, 2004).
- Berelson, W.M., Hammond, D.E., O'Neill, D., Xu, X.-M., Chin, C., Zuehlke, J., 1990. Benthic fluxes and pore water studies from sediments of the central equatorial North Pacific: nutrient diagenesis. *Geochim. Cosmochim. Acta* 54, 3001–3012.
- Berner, R.A., 1980. *Early Diagenesis – A Theoretical Approach*. Princeton University Press, Princeton, NJ, p. 241.
- Blankenship, L.E., Yayanos, A.A., Cadien, D.B., Levin, L.A., 2006. Vertical zonation patterns of scavenging amphipods from the Hadal zone of the Tonga and Kermadec Trenches. *Deep Sea Res. I* 53, 48–63.
- Blankenship-Williams, L.E., Levin, L.A., 2009. Living deep: a synopsis of hadal trench ecology. *Mar. Technol. Soc. J.* 43 (5), 137–143.
- Boudreau, B.P., 1997. *Diagenetic Models and Their Implementation*. Springer-Verlag, N.Y., p. 415.
- Canfield, D.E., 1994. Factors influencing organic carbon preservation in marine sediments. *Chem. Geol.* 114, 315–329.
- Carreira, C., Staal, M., Middelboe, M., Brussaard, C.P.D., 2015. Counting viruses and bacteria in photosynthetic microbial mats. *Appl. Environ. Microbiol.* 81, 2149–2155.
- Cui, W., Hu, Y., Guo, W., Pan, B., Wang, F., 2014. Reprint of a preliminary design of a movable laboratory for hadal trenches. *Methods Oceanogr.* 10, 178–193.
- Danovaro, R., Middelboe, M., 2010. *Manual of aquatic viral. In: Wilhelm, S.W., Weinbauer, M.G., Suttle, C.A. (Eds.), Ecology*, pp. 74–81.
- Danovaro, R., Gambi, C., Della Croce, N., 2002. Meiofauna hotspot in the Atacama Trench, eastern South Pacific Ocean. *Deep Sea Res. I* 49 (5), 843–857.
- Danovaro, R., Croce, N.D., Dell'Anno, A., Pusceddu, A., 2003. A depocenter of organic matter at 7800 m depth in the SE Pacific Ocean. *Deep Sea Res. I* 50, 1411–1420.
- DeLong, E.F., Franks, D.G., Yayanos, A.A., 1997. Evolutionary relationships of cultivated psychrophilic and barophilic deep sea bacteria. *Appl. Environ. Microbiol.* 63, 2105–2108.
- Fischer, J.P., Ferdelman, T., D'Hondt, S., Roy, H., Wenzhöfer, F., 2009. Oxygen penetration deep into the sediment of the South Pacific gyre. *Biogeosciences* 6, 1467–1478.
- Fisher, R.L., 1954. On the sounding of trenches. *Deep Sea Res.* 2, 48–58.
- Fujii, T., Kilgallen, N.M., Rowden, A.A., Jamieson, A.J., 2013. Deep sea amphipod community structure across abyssal to hadal depths in the Peru–Chile and Kermadec trenches. *Mar. Ecol. Prog. Ser.* 492, 125–138.
- Gallo, N.D., Cameron, J., Hardy, K., Fryer, P., Bartlett, D.H., Levin, L.A., 2015. Submersible- and lander-based community patterns in the Mariana and New Britain trenches: influence of productivity and depth on epibenthic and scavenging communities. *Deep Sea Res. I* 99, 119–133.
- Glud, R.N., 2008. Oxygen dynamics in marine sediments. *Mar. Biol.* 154, 243–289.
- Glud, R.N., Gundersen, J.K., Holby, O., 1999. Benthic in situ respiration in the upwelling area off central Chile. *Mar. Ecol. Prog. Series* 180, 7–21.
- Glud, R.N., Gundersen, J.K., Jørgensen, B.B., Revsbech, N.P., Schulz, H.D., 1994. Diffusive and total oxygen uptake of deep sea sediments in the eastern South Atlantic Ocean: in situ and laboratory measurements. *Deep Sea Res. I* 41,

- 1767–1788.
- Glud, R.N., Wenzhöfer, F., Tengberg, A., Middelboe, M., Oguri, K., Kitazato, H., 2005. Distribution of oxygen in surface sediments from central Sagami Bay, Japan: in situ measurements by microelectrodes and planar optodes. *Deep Sea Res. I* 52, 1974–1987.
- Glud, R.N., Stahl, H., Berg, P., Wenzhöfer, F., Oguri, K., Kitazato, H., 2009. In situ microscale variation in distribution and consumption of O<sub>2</sub>: a case study from a deep ocean margin sediment (Sagami Bay, Japan). *Limnol. Oceanogr.* 54 (1), 1–12.
- Glud, R.N., Wenzhöfer, F., Middelboe, M., Oguri, K., Turnewitsch, R., Canfield, D.E., Kitazato, H., 2013. High rates of microbial carbon turnover in sediments in the deepest oceanic trench on Earth. *Nat. Geosci.* 6, 284–288.
- Gooday, A.J., Uematsu, K., Kitazato, H., Toyofuku, T., Young, J.R., 2010. Traces of dissolved particles, including coccoliths, in the tests of agglutinated foraminifera from the challenger deep (10,897 m water depth, western equatorial Pacific). *Deep Sea Res. I* 57, 239–247.
- Grasshoff, K., 1983. Determination of oxygen. In: Grasshoff, K., Ehrhardt, M., Kremling, K. (Eds.), *Methods of Seawater Analysis*. Verlag Chemie, Weinheim, pp. 61–72.
- Gundersen, J.K., Ramsing, N.B., Glud, R.N., 1998. Predicting the signal of O<sub>2</sub> micro-sensors from physical dimensions, temperature, salinity, and O<sub>2</sub> concentration. *Limnol. Oceanogr.* 43, 1932–1937.
- Hales, B., Emerson, S., Archer, D., 1994. Respiration and dissolution in the sediments of the western North Atlantic: estimates from models of in situ microelectrode measurements of pore water oxygen and pH. *Deep Sea Res. I* 41, 695–719.
- Hall, P.O.J., Brunnegard, J., Hulthe, G., Martin, W.R., Stahl, H., Tengberg, A., 2007. Dissolved organic matter in abyssal sediments; core recovery artifacts. *Limnol. Oceanogr.* 52, 19–31.
- Ichino, M.C., Clark, M.R., Drzen, J.C., Jamieson, A., Jones, D.O.B., Martin, A.P., Rowden, A.A., Shank, T.M., Yancey, P.H., Ruhl, H.A., 2015. The distribution of benthic biomass in hadal trenches: a modelling approach to investigate the effect of vertical and lateral organic matter transport to the seafloor. *Deep Sea Res. I* 100, 21–33.
- Itou, M., Matsumura, I., Noriki, S., 2000. A large flux of particulate matter in the deep Japan Trench observed just after the 1994 Sanriku-Oki earthquake. *Deep Sea Res. I* 47, 1987–1998.
- Jahnke, R.A., 1996. The global ocean flux of particulate organic carbon: areal distribution and magnitude. *Glob. Biogeochem. Cycles* 10, 71–88.
- Jahnke, R.A., Jackson, G.A., 1992. The spatial distribution of sea floor oxygen consumption in the Atlantic and Pacific Ocean. In: Rowe, G.T., Pariente, V. (Eds.), *Deep Sea Food Chains and the Global Carbon Cycle*. Kluwer Academic, Dordrecht, pp. 295–308.
- Jahnke, R.A., Reimers, C.E., Craven, D.B., 1990. Intensification of recycling of organic matter at the sea floor near ocean margins. *Nature* 348, 50–54.
- Jamieson, A. (Ed.), 2015. *The Hadal Zone – Life in the Deepest Ocean*. Cambridge University Press, Cambridge, p. 372.
- Jamieson, A.J., Fujii, T., Solan, M., Priede, I.G., 2009. HADEEP: free-falling landers to the deepest places on earth. *Mar. Technol. Soc. J.* 43 (5), 151–160.
- Jamieson, A.J., Fujii, T., Mayor, D.J., Solan, M., Priede, I.G., 2010. Hadal trenches: the ecology of the deepest places on earth. *Trends Ecol. Evol.* 25, 190–197.
- Jumars, P.A., Hessler, R.R., 1976. Hadal community structure: implications from the Aleutian Trench. *J. Mar. Res.* 34, 547–560.
- Kato, C., 2011. Distribution of piezophiles. In: Horikoshi, K., Antranikian, G., Bull, A. T., Robb, F.T., Stetter, K.O. (Eds.), *Extremophiles Handbook*. Springer, London, pp. 644–653.
- Kawamura, K., Sasaki, T., Kanamatsu, T., Sagaguchi, A., Ogawa, Y., 2012. Large submarine landslides in the Japan Trench: a new scenario for additional tsunami generation. *Geophys. Res. Lett.* . <http://dx.doi.org/10.1029/2011GL050661>
- Kitahashi, T., Kawamura, K., Kojima, S., Shimanaga, M., 2013. Assemblage gradually change from bathyal to hadal depth: a case study on harpacticoid copepods around the Kuril Trench (north-west Pacific Ocean). *Deep Sea Res. I* 74, 39–47.
- Kristensen, E., 1988. Benthic fauna and biogeochemical processes in marine sediments: microbial activities and fluxes. In: Blackburn, T.H., Sørensen, J. (Eds.), *Nitrogen Cycling in Coastal Marine Environments*. John Wiley, New York, pp. 275–299.
- Leduc, D., Rowden, A.A., Glud, R.N., Wenzhöfer, F., Kitazato, H., Clark, M.R., 2016. Comparison between infaunal communities of the deep floor and edge of the Tonga Trench: possible effects of differences in organic matter supply. *Deep-Sea Res. I* (this Issue).
- de Leo, F.C., Smith, C.R., Rowden, A.A., Bowden, D.A., Clark, M.R., 2010. Submarine canyons: hotspots of benthic biomass and productivity in the deep sea. *Proc. R. Soc. B* 277, 2783–2792. <http://dx.doi.org/10.1098/rspb.2010.0462>.
- Murashima, T., Nakajoh, H., Takami, H., Yamauchi, N., Miura, A., Ishizuka, H., 2009. 11,000 m Class free fall mooring system. In: *Proceedings of the OCEANS 2009-EUROPE*, 2009. OCEANS '09, pp. 1–5.
- Murray, J.W., Grundmanis, V., 1980. Oxygen consumption in Pelagic Marine sediments. *Science* 209, 1527–1530.
- Nozaki, Y., Ohta, Y., 1993. Rapid and frequent turbidite accumulation in the bottom of Izu-Ogasawara Trench: chemical and radiochemical evidence. *Earth Planet. Sci. Lett.* 120, 345–360.
- Nunoura, T., Takaki, Y., Hirai, M., Shimamura, S., Makabke, A., Koide, O., Kikuchi, T., Miyazaki, J., Koba, K., Yoshida, N., Sunamura, M., Takai, K., 2015. Hadal biosphere: Insight into the microbial ecosystem in the deepest ocean on Earth. *Proc. Natl. Acad. Sci.* 112 (11), E1230–E1236. <http://dx.doi.org/10.1073/pnas.1421816112>.
- Ogawa, Y., Takami, Y., Takazawa, S., 2008. Oblique subduction in an island arc collision setting: unique sedimentation, accretion, and deformation processes in the Boso TTT-type triple junction area, NW Pacific. In: Draut, A.E., Clift, P.D., Scholl, D.W. (Eds.), *Formation and Applications of the Sedimentary Record in Arc Collision Zones 436*. Geological Society of America Special Paper, pp. 155–170. [http://dx.doi.org/10.1130/2008.2436\(07\)](http://dx.doi.org/10.1130/2008.2436(07)).
- Oguri, K., Kawamura, K., Sakaguchi, A., Toyofuku, T., Kasaya, T., Murayama, M., Fujikura, K., Glud, R.N., Kitazato, H., 2013. Hadal disturbance in the Japan Trench as induced by the 2011 Tohoku-Oki Earthquake. *Sci. Rep.* 3, 1915. <http://dx.doi.org/10.1038/srep01915>.
- Pastor, L., Deflandre, B., Viollier, E., Cathalot, C., Metzger, E., Rabouille, C., Escoubeyrou, K., Lloret, E., Pruski, A.M., Vétion, G., Desmalades, M., Buscail, R., Grémare, A., 2011. Influence of the organic matter composition on benthic oxygen demand in the Rhône River prodelta (NW Mediterranean Sea). *Cont. Shelf Res.* 31, 1008–1019.
- Reimers, C.E., Fischer, K.M., Merewether, R., Smith, K.L., Jahnke, R.A., 1986. Oxygen microprofiles measured in situ in deep ocean sediments. *Nature* 320, 741–744.
- Renard, V., Nakamura, K., Angelier, J., Azema, J., Bourgois, J., Deplus, C., Fujioka, K., Hamano, Y., Huchon, P., Kinoshita, H., Labaume, P., Ogawa, Y., Seno, T., Takeuchi, A., Tanahashi, M., Uchiyama, A., Vignerresse, J.-L., 1987. Trench triple junction off Central Japan – preliminary results of French-Japanese 1984 Kaiko cruise, Leg 2. *Earth Planet. Sci. Lett.* 83, 243–256.
- Revsbech, N.P., 1989. An oxygen microsensor with a guard cathode. *Limnol. Oceanogr.* 34, 474–478.
- Shuman, F.R., Lorenzen, C.J., 1975. Quantitative degradation of chlorophyll by marine herbivore. *Limnol. Oceanogr.* 20 (4), 580–586.
- Smith, K.L., White, G.A., Laver, M.B., 1978. Oxygen uptake and nutrient exchange of sediments measured in situ using a free vehicle grab respirometer. *Deep Sea Res.* 26 (337–246).
- Smith, K.L., Ruhl, H.A., Kahru, M., Huffard, C.L., Sherman, A.D., 2013. Deep ocean communities impacted by changing climate over 24 y in the abyssal northeast Pacific Ocean. *Proc. Natl. Acad. Sci.* 110, 19838–19841.
- Somero, G.N., 1992. Adaptations to high hydrostatic pressure. *Annu. Rev. Physiol.* 54, 557–577.
- Stephens, M.P., Kadko, D.C., Smith, C.R., Latasa, M., 1997. Chlorophyll-a and pheopigments as tracers of labile organic carbon at the central equatorial Pacific seafloor. *Geochim. Cosmochim. Acta* 61 (21), 4605–4619.
- de Stigter, H.C., Wim, B., de Jesus Mendes, P.A., César Jesus, C., Thomsen, L., van den Bergh, G.D., van Weering, T.C.E., 2007. Recent sediment transport and deposition in the Nazaré Canyon, Portuguese continental margin. *Mar. Geol.* 246 (144.164).
- Swinbanks, D.D., Shirayama, Y., 1986. High levels of natural radionuclides in a deep sea infaunal xenophyophore. *Nature* 320, 354–358.
- Tamburini, C., Boutfir, M., Garel, M., Colwell, R.R., Deming, J.W., 2013. Prokaryotic responses to hydrostatic pressure in the ocean – a review. *Environ. Microbiol.* 15 (5), 1262–1274.
- Tietjen, J.H., Deming, J.W., Rowe, G.T., Macko, S., Wilke, R.J., 1989. Meiobenthos of the Hatteras abyssal-plain and Puerto-Rico trench – abundance, biomass and association with bacteria and particulate fluxes. *Deep Sea Res. Part A* 36 (10), 1567–1577.
- Todo, Y., Kitazato, H., Hashimoto, J., Gooday, A.J., 2005. Simple Foraminifera flourish at the oceans deepest point. *Science* 307, 689–690.
- Tsumune, D., Aoyama, M., Hirose, K., Bryan, F.O., Lindsay, K., Danabasoglu, G., 2011. Transport of <sup>137</sup>Cs to the Southern Hemisphere in an ocean general circulation model. *Prog. Oceanogr.* 89, 38–48.
- Turnewitsch, R., Falahat, S., Stehlikova, J., Oguri, K., Glud, R.N., Middelboe, M., Kitazato, H., Wenzhöfer, F., Ando, K., Fujio, S., Yanagimoto, D., 2014. Recent sediment dynamics in hadal trenches: evidence for the influence of higher frequency (tidal, near-inertial) fluid dynamics. *Deep Sea Res. I* 90, 125–138.
- Verado, D.J., Froelich, P.N., McIntyre, A., 1990. Determination of organic carbon and nitrogen in marine sediment using the Carlo Erba NA-1500. *Anal. Deep Sea Res.* 37, 157–165.
- Wenzhöfer, F., Glud, R.N., 2002. Benthic carbon mineralization in the Atlantic: a synthesis based on in situ data from the last decade. *Deep Sea Res. I* 49, 1255–1279.
- Wenzhöfer, F., Glud, R.N., 2004. Small-scale spatial and temporal variability in coastal benthic O<sub>2</sub> dynamics: effects of fauna activity. *Limnol. Oceanogr.* 49 (5), 1471–1481.
- Wollast, R., 1998. Evaluation and comparison of the global carbon cycle in the coastal zone and in the open ocean. In: Brink, K.H., Robinson, A.R. (Eds.), *The Sea: The Global Coastal Ocean: Processes and Methods*. John Wiley & Sons, New York, pp. 213–252.
- Yamada, M., Kitaoka, H., Tsunogai, S., 1983. A radiochemical study of sedimentation onto the Japan Trench floor. *Deep Sea Res.* 30 (11A), 1147–1156.